AIP | APL Materials

Field-effect and capacitive properties of water-gated transistors based on polythiophene derivatives

R. Porrazzo, S. Bellani, A. Luzio, C. Bertarelli, G. Lanzani, M. Caironi, and M. R. Antognazza

Citation: APL Mater. **3**, 014905 (2015); doi: 10.1063/1.4900888
View online: http://dx.doi.org/10.1063/1.4900888
View Table of Contents: http://scitation.aip.org/content/aip/journal/aplmater/3/1?ver=pdfcov
Published by the AIP Publishing

Field-effect and capacitive properties of water-gated transistors based on polythiophene derivatives

R. Porrazzo,[1,2] S. Bellani,[1,2] A. Luzio,[1] C. Bertarelli,[1,3] G. Lanzani,[1,2] M. Caironi,[1,a] and M. R. Antognazza[1,a]
[1]*Center for Nano Science and Technology @PoliMi, Istituto Italiano di Tecnologia, Via Pascoli 70/3, 20133 Milan, Italy*
[2]*Dipartimento di Fisica, Politecnico di Milano, P.zza L. da Vinci 32, 20133 Milan, Italy*
[3]*Dipartimento di Chimica, Materiali e Ingegneria Chimica "G. Natta," Politecnico di Milano, P.zza L. Da Vinci 32, 20133 Milan, Italy*

(Received 1 September 2014; accepted 22 October 2014; published online 10 November 2014)

Recently, water-gated organic field-effect transistors (WGOFET) have been intensively studied for their application in the biological field. Surprisingly, a very limited number of conjugated polymers have been reported so far. Here, we systematically explore a series of polythiophene derivatives, presenting different alkyl side chains lengths and orientation, and characterized by various morphologies: comparative evaluation of their performances allows highlighting the critical role played by alkyl side chains, which significantly affects the polymer/water interface capacitance. Reported results provide useful guidelines towards further development of WGOFETs and represent a step forward in the understanding of the polymer/water interface phenomena. [http://dx.doi.org/10.1063/1.4900888]

Water-gated organic field-effect transistors (WGOFETs) are transistors where an electrolyte, in particular an aqueous saline solution, is utilized as the gating medium. WGOFETs are characterized by distinctive features: they allow low-voltage operation (<1 V), due to the large electric double layer capacitance developed at the liquid-semiconductor interface; they are suitable for small scale integration with *in-vitro* systems, and, thanks to the operation in physiological solutions, where biorecognition elements are active, they are particularly suitable for biological applications as biosensors and biotransducers.[1–4]

Conjugated semiconductors offer peculiar characteristics for the use in WGOFETs. They can be processed from solution at low temperature, thus enabling large-area processing on flexible substrates, thanks to high-throughput printing techniques.[5–8] Moreover, organic semiconductors offer advantages in terms of bio-compatibility[9,10] and their surfaces can be chemically modified to anchor bio-recognition elements, allowing effective bio-sensing.[11–13] In particular, semiconducting polymers are mechanically robust, enable the control of solutions rheology, and allow easier uniform depositions with respect to small molecules.

The choice of the semiconducting polymer to be used as active material in liquid-gated configurations is of crucial importance to fabricate WGOFET devices with good electronic performances. Poly-3-hexylthiophene (P3HT) has been the first material to be demonstrated and widely reported in WGOFETs configurations.[14,15] Recently, we reported a higher performances WGOFET based on poly(2,5-bis(3-hexadecylthiophen-2-yl)thieno[3,2-b]thiophene) (pBTTT) as semiconducting layer.[16] The device showed relatively high charge carriers mobility (0.08 cm^2/Vs), at levels comparable with single-crystal based water gated transistors, and improved electro-chemical stability. In addition, the device showed very good transistor behavior also when gated with a saline

[a]Authors to whom correspondence should be addressed. Electronic addresses: mario.caironi@iit.it and mariarosa.antognazza@iit.it

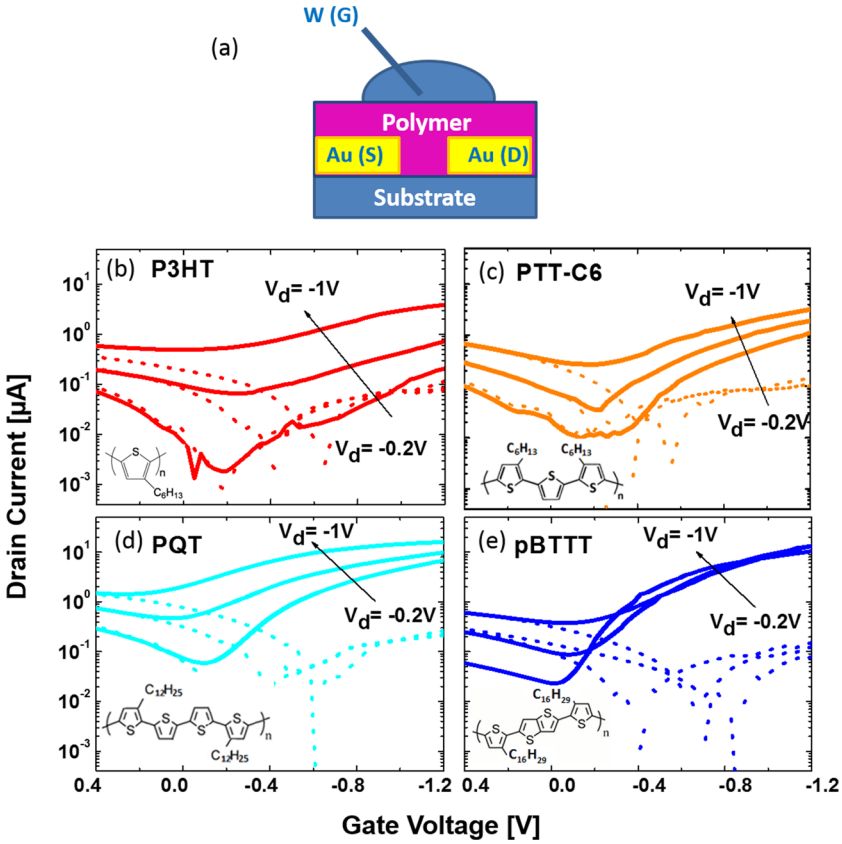

FIG. 1. (a) Represents the schematic section of a WGOFET device. Transfer characteristics of WGOFET devices based on (b) regioregular P3HT, (c) poly-terthiophene PTT-C6, (d) poly-quaterthiophene PQT, and (e) pBTTT. Solid and dashed lines represent the source-drain and leakage currents of each device, respectively. Chemical structures of the polymers are reported in the inset of the correspondent characteristics.

solution up to 0.2 M concentration, thus paving the way for bio-sensing applications based on a simple device structure.

Despite these recent examples, the number of polymers demonstrated to function in water-gated devices is still scarce, and even less information is available for gating through physiological-like media, necessary for future applications.

The goal of this work is to explore a polythiophene derivatives series with the aim to widen the class of organic semiconducting materials employable as active layers, to test the possibility of operating in saline aqueous solutions and, based on detailed comparison of their performances, to identify what are the critical parameters governing their functioning in a WGOFET configuration. The series is based on polymers sharing a polythiophene backbone; polythiophenes already demonstrated their superior stability properties in a physiological environment, in a variety of different biological preparations and applications;[17–19] indeed, the vast majority of WGOFET devices reported so far is based on polymers belonging to this material class. Moreover, polythiophenes are considered benchmark candidates for the fine tuning of chemical structures.[20] We have constructed the series by employing P3HT (Fig. 1(b)) and pBTTT (Fig. 1(e)) as useful benchmark cases, and we have explored two additional regiodefined polythiophene derivatives, characterized either by three or four thiophenes in the repeating unit and by different lengths of the alkyl chains. Besides demonstrating their good performances in a WGOFETs configuration, we investigate the mobility-capacitance product for the whole series, one of the most relevant figures of merits sizing the channel currents in water-gated devices. The comparative study performed here allowed highlighting the specific role played by the double-layer capacitance at the semiconductor-electrolyte interface, as determined by a specific orientation of the polymer alkyl-side chains at the interface with water. We provide important indications

for the understanding of the water-polymer interface, and useful guidelines towards a further development of WGOFETs for biosensing.

The chemical structures of the considered *p*-type organic semiconductors used in this study are shown in the inset of Figures 1(b)–1(e). Regio-regular P3HT (average M_w 53 000 g/mol, Figure 1(b), was purchased from Sigma–Aldrich, and used without any further purification. Figure 1(c) shows poly-3,3″-dihexyl-2,2′:5′,2″-terthiophene (3,3″-DHTT), consisting of terthiophenes bearing alkyl chains with six carbon atoms: it is therefore referred to as PTT-C6 (average M_w is 25 800 g/mol, as determined by gel permeation chromatography in tetrahydrofuran at 35 °C using polystyrene as standard). PTT-C6 was synthesized for this work following the general procedure reported in Ref. 21, which consists in the oxidative polymerization of the 3,3″ dialkyl-2,2′-5′-2′-terthiophene by $FeCl_3$ in $CHCl_3$ at 40 °C. Chemical structure of poly[5,5′-bis(3-alkyl-2-thienyl)-2,2′-bithiophene] (PQT, purchased from American Dye Source, average M_w 40 000 g/mol) and pBTTT (from Ossila, Ltd., M_w 82 000 g/mol), is shown in Figures 1(d) and 1(e).

In Figure 1(a), a schematic representation of the WGOFET architecture is reported. The adopted transistors geometry is Top-Gate, Bottom-Contact, fabricated starting from a glass substrate, with photolithographically defined Source (S) and Drain (D) gold electrodes. The transistor channel length and width are $L = 40$ μm and $W = 20$ mm, respectively. All semiconductors are deposited by spin coating from solution directly on the electrodes. P3HT is dissolved in chloroform at a concentration of 3 mg ml^{-1}, while the other polymers are deposited from dichlorobenzene solutions at a concentration of 5 mg ml^{-1}. Films are deposited by spin-coating to achieve a final thickness in the order of 70 nm. After spin coating, pBTTT films are annealed at 80 °C for 10 min for solvent removal, then up to 180 °C for 10 min, to activate the liquid crystalline phase transition.[22] All other polythiophene semiconductors undergo a thermal treatment at 120 °C for 20 min.

A drop of purified tap water (Milli-Q® water system, Millipore) or aqueous saline solution (sodium chloride NaCl, 0.2 M concentration), acting as electrolyte media, is put directly in contact with the semiconductor, on top of the transistor channel area. The average volume of the water drop is 2.1 mm^3, corresponding to the volume of a semi-sphere of diameter of 2 mm. Finally, the gate voltage is applied to the system through a tungsten tip immersed in water and placed at a fixed distance of 0.75 mm from the polymer. Reference OFETs with a polymer dielectric are also realized, employing 500 nm of polymethylmethacrylate (PMMA) as the insulating layer, deposited by spin-coating on top of the semiconductor layer, and 40 nm thick evaporated Al electrodes as gate contacts. The water-gated transistor characterization is performed in ambient air with an Agilent B1500A semiconductor parameter analyzer, while the polymer dielectric devices are tested in a nitrogen glovebox. The transistor field-effect mobility μ_{sat} and on/off ratio are extracted from the characteristics in the saturation regime. The electrochemical characterization is carried out through electrochemical impedance spectroscopy (EIS) with a potentiostat (Metrohm Autolab PGstat 302). EIS is performed on Au/water/polymer/Au capacitors structures, in a two electrodes configuration (polymer/gold interface area ~5 mm^2; gold counter electrode area ~9 cm^2), and Nova 1.8 software is employed for data analysis. Measurements are carried out in the frequency range from 0.3 Hz to 50 kHz, by applying a sine wave signal of 0.02 V rms amplitude, while the DC voltage, referred to the gold counter electrode, ranges from 0 V to −0.9 V with −0.3 V steps. For the details of the equivalent electrical circuit used to fit the EIS data please refer to the supplementary material.[23] OCA-15 Optical Contact Angle Measuring Instrument (Dataphysics) is employed to measure the water Contact Angle (CA) on the polymer films surface before and after immersion in purified water. The topography characterization of the polymer films is obtained with an Agilent 5500 Atomic Force Microscope (AFM) in acoustic mode.

All polymers in the series were at first tested by EIS technique in Au/water/polymer/Au capacitors structures, in order to characterize the voltage and frequency dependence of the double layer capacitance developing at the semiconductor-electrolyte interface. The data of the effective capacitance, along with details of the equivalent circuit used to fit the EIS data, are reported in the supplementary material.[23] In the low frequency regime (<1 Hz), all polymers display a saturation of the effective capacitance value, indicating the building up of a Helmholtz double layer. Extracted capacitance values at 0.3 Hz (Table I) range from 0.6 μF/cm^2 for pBTTT, to 2 μF/cm^2 for P3HT and PTT-C6 systems, to 1 μF/cm^2 in PQT-based devices. All extracted capacitances fall

TABLE I. Capacitance C, mobility of the WGOFET $\mu_{\text{SAT WGOFET}}$, product $C\cdot\mu_{\text{SAT WGOFET}}$ and onset voltages V_{on} are shown in columns 1–4 for different polymers in a WGOFET configuration. Solid state mobility $\mu_{\text{SAT OFET}}$ of correspondent devices is shown in column 5. Contact angles values prior to water exposure, together with contact-angles variation values, as taken before and after exposure to water, are shown in Columns 6 and 7, respectively.

	C [μF/cm^2]	$\mu_{\text{SAT WGOFET}}$ [cm^2/Vs]	$C\cdot\mu_{\text{SAT WGOFET}}$ [μF/Vs]	V_{on} [V]	$\mu_{\text{SAT OFET}}$ [cm^2/Vs]	Initial CA [°]	Δ CA [°]
pBTTT	0.6	0.08 ± 0.001	0.05	−0.05	0.15	107	7
PQT	1	0.02 ± 0.002	0.02	0.2	0.07	107	5
PTT-C6	2	0.002 ± 0.001	0.004	−0.2	0.004	104	7
P3HT	2	0.003 ± 0.0015	0.006	−0.2	0.004	107	7

within the expected range of values that characterize hydrophobic semiconductors in contact with aqueous electrolytes, usually comprised between 0.5 μF/cm^2 and 10 μF/cm^2.[24,25] Detailed analysis of capacitance values obtained in each polymer systems will be presented hereinafter.

The occurrence of a double layer capacitance upon biasing in all systems points to the possibility of suitably inducing an accumulated channel in WGOFET architecture. Typical transfer curves of such devices are reported in Figures 1(b)–1(e). Solid and dashed lines represent source-drain and leakage currents, respectively. Transfer curves measurements are carried out by sweeping the gate–source voltage (V_{GS}) from 0.4 V to −1.2 V, at fixed drain-source voltage (V_{DS}) values (−0.2 V, −0.6 V, and −1 V). All devices show good p-type characteristics, with no measurable electron currents. The transfer characteristics are recorded at a scan rate of 530 mV/s: within this scan rate, the electrical characteristics are reproducible and no current hysteresis occurs between the forward and backward potential sweeps. Moreover, no change in the transfer curves behavior is observed in the 20 min time of contact between the polymers and water during testing.

Interestingly, the gate leakage currents of all fabricated devices show substantially the same voltage dependence and the same values in the investigated gate voltage window, in the order of $\sim 10^{-1}$ μA cm^{-2} at $V_g = -1.2$ V. Since leakage currents do not scale proportionally to the output currents, they cannot be correlated to the field-induced conductivity of the polymeric films; moreover, it is also unlikely that such leakage is dominated by defects (e.g., pinholes) of the polymeric films, which would imply substantial differences among different devices. Conversely, leakage currents seem to be a specific characteristic of the transistor geometry in contact with water, and (at the scan rate in which the characteristics are recorded) they are most probably determined by the series of the impedance of water and of the water/semiconductor interface.

The previously extracted double-layer capacitances at low frequency (0.3 Hz) are used to estimate the hole mobility values in the saturation regime, μ_{sat} (Table I). Reported μ_{sat} represents averaged values over seven transistors. For P3HT and pBTTT-based WGOFETs, we extract μ_{sat} of 0.003 cm^2/Vs and 0.08 cm^2/Vs, respectively, in line with previously reported data.[16] The transfer curves for PTT-C6 (Figure 1(c)) reveal current values and electrical performances similar to the P3HT-based system for increasing drain voltages, reaching maximum current value of 3 μA at $V_g = -1.2$ V. The estimated μ_{sat} is 0.002 cm^2/Vs. PQT devices (Figure 1(d)) exhibit p-type operation with features similar to pBTTT-based devices, reaching high current values (∼15 μA) at $V_g = -1.2$ V, and mobilities up to 0.01 cm^2/Vs.

In order to better compare the performances of the tested materials, the devices transfer curves at $V_d = -1$ V are summarized in Figure 2. It is possible to observe marked differences in the maximum drain current values I_{max}, reached by the different polymer-based devices at $V_{\text{gate}} = -1.2$ V. The current values of the different systems depend on the combined effect of mobility μ_{sat}, capacitance C, and onset voltage V_{ON} (reported in Table I, column 4). P3HT and PTT-C6 (identified by orange and red curves, respectively) show very similar transfer curves shape and current values, reflecting similar capacitance, mobility, and onset voltage values. PQT displays a double layer capacitance $C = 1$ μF/cm^2, a μ_{sat} value of 0.02 cm^2/Vs, and turns on at 0.2 V; pBTTT exhibits a lower capacitance value (0.6 μF/cm^2) and turns on at more negative values ($V_{\text{ON}} = -0.05$ V): however, higher values of mobility (0.08 cm^2/Vs) compensate for the lower capacitance and lead to similar I_{max} values of PQT.

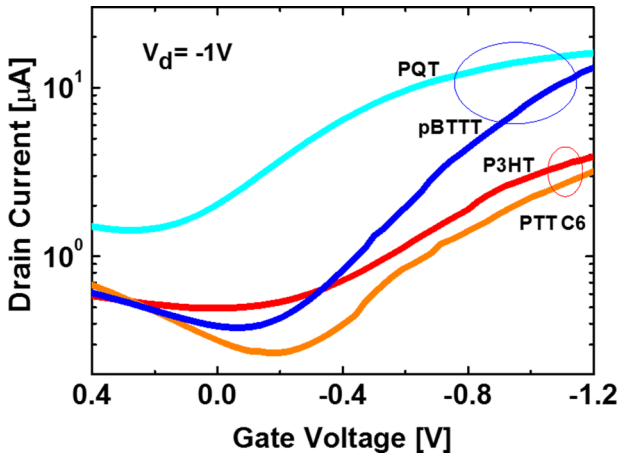

FIG. 2. Transfer characteristics comparison of the devices of Fig. 2, plotted at $V_d = -1$ V. The colour mapping discriminates different device performances: warm-colors identify lower current values of P3HT (red) and PTT-C6 (orange) transistors; cold-colors identify the higher current values of pBTTT (blue) and PQT (cyan) based-devices.

OFETs including a polymer PMMA dielectric and evaporated aluminum gate are also realized as a reference for all semiconducting materials, with the same substrates and materials processing. Transfer curves obtained in the solid-state OFET configuration are reported in the supplementary material.[23] The measured saturation mobility values are reported in Table I: μ_{SAT} for pBTTT and PQT is 0.15 cm^2/Vs and 0.07 cm^2/Vs, respectively, while for both P3HT and PTT-C6, μ_{SAT} is found to be 4×10^{-3} cm^2/Vs.

Finally, we investigated the transistors performances in a biological-like environment, gating them with 0.2 M molar concentration NaCl solutions. The transfer characteristics of the NaCl solution gated FETs are shown in Figure 3. All devices demonstrate to withstand gating with saline solution, instead of purified water, and the trend previously observed among considered materials, at a first approximation, is preserved; however, one should also note that in this case, the relative differences among considered materials are lowered. Indeed, in the presence of salt, the contribution to the current of an electrochemical component, due to polymer doping,[26,27] as well as a possible electrostatic screening exerted by ions adsorbed at the interface,[4] may play a significant role. The presence of hysteresis between the forward and backward transfer scan, not observed in devices

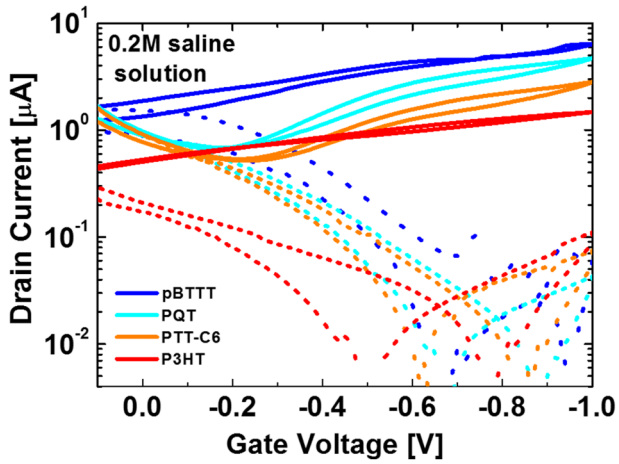

FIG. 3. Transfer characteristics comparison of the transistors gated with 0.2 M saline solution. Transcharacteristics are recorded at $V_d = -1$ V, and are reported for WGOFET devices based on PTT-C6 (orange), P3HT (red), PQT (cyan), and pBTTT (blue). Solid and dashed lines represent the source-drain and leakage currents, respectively.

gated by millipore water, indirectly supports this picture. The presence of ions is thus expected to affect the pure interaction between alkyl chains and millipore water, thus determining a modification of transfer characteristics and interface capacitance values; such a phenomenon should be taken into account in designing a complete device for biosensing, which is however beyond the goal of the present work.

In order to extrapolate guidelines for the selection and engineering of materials for water-gated transistors, our work intentionally focuses on similar polythiophenes derivatives. All considered materials show good transistor behavior, both in WGOFET and OFET configuration, however, with differences in their respective characteristics and in particular in the maximum current values reached at the highest applied gate voltage. We consider different possible conditions that might play a fundamental role in determining the overall device performances, namely: (i) surface hydrophobicity, (ii) an altered material morphology upon operation, possibly induced by prolonged contact with water; and (iii) different alkyl chain lengths, leading to different capacitance values and coupling with the water electrostatic environment. Regarding hydrophobicity, contact angle analysis is performed on the semiconducting polymers films before and after the measurement with water. All considered materials show similar static CA, around 107°, prior to water exposure, and similar variations after the functioning in WGOFET configuration (Table I, Columns 6 and 7, respectively).[28] In other words, the interaction with water is the same for all polymers under study, and cannot be at the base of a different performance. The same holds true for material morphology (ii): AFM characterization (see figures in the supplementary material[23]) shows that the films topography, different from case to case and specific for each material microstructure, is not seriously affected by the prolonged contact with water and functioning in the WGOFET configuration. Finally, we investigated (iii) the role of alkyl chain lengths, and their influence on the different measured double layer capacitances. The value of the double-layer capacitance C is a crucial parameter for the devices working in a liquid-gated configuration;[29] at variance with solid-state OFETs devices, where C is defined by the dielectric polymer thickness, in WGOFETs, the capacitance value depends on the interfacial interaction between polymer and electrolyte. The specific capacitance value, e.g., the areal capacitance, is more loosely determined by geometrical characteristics. Recently, based on results for P3HT- and pBTTT-based devices, we hypothesized the double role of the alkyl chains length and order at the semiconductor surface: first, they protect the polymer conjugated segments from the contact with the liquid; second, they are a dominant factor in sizing the interface capacitance in the case of purified water by determining the distance between the charges in the semiconductor channel and the anions in water. Bearing this model in mind, in the hypothesis of extended chains at the interface, the measured capacitance C should be related to the thickness of the alkyl chains layer d, through the relationship $C_{\text{alkyl}} = \varepsilon_{\text{r-exp}}\,\varepsilon_0/d$, where $\varepsilon_{\text{r-exp}}$ is the effective relative permittivity of the alkyl interlayer. For the polymers working in WGOFET configuration, we extract a relative permittivity value $\varepsilon_{\text{r-exp}}$ from the measured capacitance, and we compare it with the $\varepsilon_{\text{r-eff}}$ values derived from literature by taking into account different ε_{r} values for similar self-assembled monolayers, and different coverage factors[30–35] (see Table II for values, and supplementary material[23]).

The agreement between the two values is satisfactory in all cases. All in all, we can conclude that the observed WGOFETs performances of the considered polytiophene derivatives are successfully explained within the proposed model, thus confirming the key role of alkyl side chains at the interface with water.

In summary, results presented in this work confirm the suitability of polythiophenes for applications in WGOFET devices. Within the studied series, where both the repeating backbone unit and

TABLE II. Comparison between the experimentally derived values of alkyl layer relative permittivity, $\varepsilon_{\text{r-exp}}$, and the values derived from literature data $\varepsilon_{\text{r-eff}}$, calculated for all polymers working in a WGOFET configuration.

	P3HT	PTT-C6	PQT	pBTTT
$\varepsilon_{\text{r-exp}}$	1.80	1.82	1.94	1.55
$\varepsilon_{\text{r-eff}}$	1.86	1.7	1.8	1.64

alkyl chains have been modulated, PTT-C6 based devices gated with purified water show similar field-effect mobility (0.002 cm^2/Vs) and specific capacitance (2 $\mu F/cm^2$) to the ones based on P3HT, and therefore lead to similar device characteristics. In line with results on pBTTT, PQT based devices show instead a lower capacitance (1 $\mu F/cm^2$) in exactly the same device configuration, but an order of magnitude higher mobility (0.02 cm^2/Vs), resulting in improved on-currents. Very importantly, this investigation allowed us to confirm the importance of the alkyl side chains length in establishing a different interaction with the aqueous environment, affecting in a substantial way the interface capacitance and possibly providing a different protection action for polymer backbones against water penetration. Moreover, all polymers in the studied series show good performances in a biological-like environment reproduced by gating the semiconductors with 0.2 M NaCl water solution, representing the first necessary step towards the realization of a complete polymer-based biosensor, selective to specific analytes. All in all, our work highlights important conditions governing the overall functioning of WGOFET devices, thus providing useful guidelines for further improvement of their performances, through targeted chemical engineering and materials design. More generally, it also provides new insights towards the understanding of polymer/water interfaces, currently object of intense investigation.

M. R. A. and G. L. acknowledge financial support from European Union through projects PHOCS, ENERGY 2012-10.2.1, Future Emerging Technologies Collaborative Project, Grant No. 309223, and OLIMPIA, FP7-PEOPLE-212-ITN, Grant No. 316832, and support from National Grants Telethon Italy (Grant Nos. GGP12033 and GGP14022) and from Fondazione Cariplo (Grant No. 2013-0738). M.C. acknowledges financial support from European Union through the Marie-Curie Career Integration Grant 2011 "IPPIA," within the European Union Seventh Framework Programme (FP7/2007-2013) under Grant Agreement No. PCIG09-GA-2011-291844.

[1] K. Svennersten, K. C. Larsson, M. Berggren, and A. Richter-Dahlfors, Biochim. Biophys. Acta **1810**, 276 (2011).
[2] P. Lin and F. Yan, Adv. Mater. **24**, 34 (2012).
[3] L. Torsi, M. Magliulo, K. Manoli, and G. Palazzo, Chem. Soc. Rev. **42**, 8612 (2013).
[4] T. Cramer, A. Campana, F. Leonardi, S. Casalini, A. Kyndiah, M. Murgia, and F. Biscarini, J. Mater. Chem. B **1**, 3728 (2013).
[5] K.-J. Baeg, M. Caironi, and Y.-Y. Noh, Adv. Mater. **25**, 4210 (2013).
[6] S. H. Kim, K. Hong, W. Xie, K. H. Lee, S. Zhang, T. P. Lodge, and C. D. Frisbie, Adv. Mater. **25**, 1822 (2013).
[7] A. C. Arias, D. MacKenzie, I. McCullogh, J. Rivnay, and A. Salleo, Chem. Rev. **110**, 3 (2010).
[8] H. Sirringhaus, M. Bird, and N. Zhao, Adv. Mater. **22**, 3893 (2010).
[9] G. Scarpa, A.-L. Idzko, A. Yadav, and S. Thalhammer, Sensors **10**, 2262 (2010).
[10] D. Ghezzi, M. R. Antognazza, R. Maccarone, S. Bellani, E. Lanzarini, N. Martino, M. Mete, G. Pertile, S. Bisti, G. Lanzani, and F. Benfenati, Nat. Photonics **7**, 400 (2013).
[11] C. Suspène, B. Piro, S. Reisberg, M.-C. Pham, H. Toss, M. Berggren, A. Yassar, and G. Horowitz, J. Mater. Chem. B **1**, 2090 (2013).
[12] L. Kergoat, B. Piro, M. Berggren, M. C. Pham, A. Yassar, and G. Horowitz, Org. Electron. **13**, 1 (2012).
[13] M. Magliulo, A. Mallardi, M. Y. Mulla, S. Cotrone, B. R. Pistillo, P. Favia, I. Vikholm-Lundin, G. Palazzo, and L. Torsi, Adv. Mater. **25**, 2090 (2013).
[14] L. Kergoat, L. Herlogsson, D. Braga, B. Piro, M.-C. Pham, X. Crispin, M. Berggren, and G. Horowitz, Adv. Mater. **22**, 2565 (2010).
[15] S. Cotrone, M. Ambrico, H. Toss, M. D. Angione, M. Magliulo, A. Mallardi, M. Berggren, G. Palazzo, G. Horowitz, T. Ligonzo, and L. Torsi, Org. Electron. **13**, 638 (2012).
[16] R. Porrazzo, S. Bellani, A. Luzio, E. Lanzarini, M. Caironi, and M. R. Antognazza, Org. Electron. **15**, 2126 (2014).
[17] V. Benfenati, N. Martino, M. R. Antognazza, A. Pistone, S. Toffanin, S. Ferroni, G. Lanzani, and M. Muccini, Adv. Healthcare Mater. **3**, 306 (2014).
[18] G. Scarpa, A.-L. Idzko, S. Götz, and S. Thalhammer, Macromol. Biosci. **10**, 378 (2010).
[19] D. Khodagholy, T. Doublet, P. Quilichini, M. Gurfinkel, P. Leleux, A. Ghestem, E. Ismailova, T. Hervé, S. Sanaur, C. Bernard, and G. Malliaras, Nat. Commun. **4**, 1575 (2013).
[20] G. Barbarella, M. Melucci, and G. Sotgiu, Adv. Mater. **13**, 1581 (2005).
[21] M. C. Gallazzi, C. Bertarelli, and E. Montoneri, Synth. Met. **128**, 91 (2002).
[22] I. Mc Culloch, M. Heeney, C. Bailey, K. Genevicius, I. MacDonald, M. Shkunov, D. Sparrowe, S. Tierney, R. Wagner, W. Zhang, M. L. Chabinyc, R. J. Kline, M. D. McGehee, and M. F. Toney, Nat. Mater. **5**, 328 (2006).
[23] See supplementary material at http://dx.doi.org/10.1063/1.4900888 for additional details and Figs. SI1, SI2, SI3, and SI4.
[24] H. Toss, C. Suspène, B. Piro, A. Yassar, X. Crispin, L. Kergoat, M.-C. Pham, and M. Berggren, Org. Electron. **15**, 2420 (2014).
[25] J. A. Garrido, S. Nowy, A. Härtl, and M. Stutzmann, Langmuir **24**, 9898 (2008).
[26] E. Stavrinidou, M. Sessolo, B. Winther-Jensen, S. Sanaur, and G. Malliaras, AIP Adv. **4**, 017127 (2014).
[27] J. Lee, L. G. Kaake, J. H Cho, X.-Y. Zhu, T. P. Lodge, and C. D. Frisbie, J. Phys. Chem. C **113**, 8972 (2009).
[28] S. Bellani, D. Fazzi, P. Bruno, E. Giussani, E. Canesi, G. Lanzani, and M. R. Antognazza, J. Phys. Chem. C **118**, 6291 (2014).

[29] A. Bard and I. Faulkner, *Electrochemical Methods: Fundamentals and Applications* (Wiley, New York, 2001).
[30] O. S. Beng, W. Yiliang, L. Ping, and S. Gardner, Adv. Mater. **17**, 1141 (2005).
[31] P. Keg, A. Lohani, D. Fichou, Y. M. Lam, Y. Wu, B. S. Ong, and S. G. Mhaisalkar, Macromol. Rapid Commun. **29**, 1197 (2008).
[32] M. C. Gallazzi, L. Catellani, R. A. Marin, and G. Zerbi, J. Polym. Sci., Part A: Polym. Chem. **31**, 3339 (1993).
[33] J. E. Northrup, M. L. Chabinyc, R. Hamilton, I. McCulloch, and M. Heeney, J. Appl. Phys. **104**, 083705 (2008).
[34] B. Fabre, J. Hauquier, and P. Allongue, J. Electroanal. Chem. **629**, 63 (2009).
[35] A. Ulman, Chem. Rev. **96**, 1533 (1996).